



## Advances in Water in Agrosience

# Impacts of irrigation development on water quality in the San Salvador watershed (Part 1): Assessment of current nutrient delivery and transport using SWAT

**Impactos del desarrollo del riego en la calidad de agua en la cuenca del río San Salvador (Parte 1): Análisis de la exportación y el transporte de nutrientes actuales mediante SWAT**

**Impactos do desenvolvimento da irrigação na qualidade da água na bacia hidrográfica de San Salvador (Parte 1): Análise da exportação e do transporte atuais de nutrientes usando o SWAT**

Hastings, F. <sup>1</sup>; Pérez-Bidegain, M. <sup>1</sup>; Navas, R. <sup>2</sup>; Gorgoglione, A. <sup>3</sup>

<sup>1</sup>Universidad de la República, Facultad de Agronomía, Montevideo, Uruguay

<sup>2</sup>Universidad de la República, Centro Universitario Regional Norte, Departamento del Agua, Salto, Uruguay

<sup>3</sup>Universidad de la República, Facultad de Ingeniería, Montevideo, Uruguay

### Editor

Pablo Gamazo   
Universidad de la República,  
Salto, Uruguay

Received 17 May 2023

Accepted 23 Oct 2023

Published 06 Feb 2024

### Correspondence

Florencia Hastings  
ing.fhastings@gmail.com

## Abstract

The development of irrigation involves a change in land use and management and has implications for water quality and quantity. It is critical to design conservation practices and best management practices consistent with sustainable agricultural intensification. The objective of this work was to understand and characterize key processes affecting hydrology, nutrient export and transport, and quantify impacts in the San Salvador watershed. For such purpose, the Soil & Water Assessment Tool (SWAT) was implemented, calibrated for water quantity, and water quality was adjusted using soft calibration techniques. The model reproduces water quantity and nutrient balance, and aids in characterizing the nutrient delivery and transport in the watershed. The magnitude of runoff affects the balance of nutrients. In high flows, diffuse sources are more prevalent, while in low flows, point sources and direct livestock manure to the river are more significant. The main outcomes of this work contribute to the design of strategies to achieve sustainable agricultural intensification. It also describes a new modeling tool freely available that could be used in further studies.

**Keywords:** sustainable agriculture, water quality, SWAT

## Resumen

El desarrollo del riego implica un cambio en el uso y el manejo del suelo e impacta en la calidad y la cantidad de agua. Es fundamental diseñar prácticas de conservación y buenas prácticas agrícolas que respondan al paradigma de intensificación agrícola sostenible. El objetivo de este trabajo fue comprender y caracterizar los procesos claves que afectan la hidrología, la exportación y el transporte de nutrientes y cuantificar los impactos en la cuenca del río San Salvador. Se implementó el modelo Soil & Water Assessment Tool, se calibró la cantidad de agua y la calidad de agua fue ajustada utilizando técnicas de calibración blanda. El modelo reproduce adecuadamente la cantidad de agua y el balance



Hastings F, Pérez-Bidegain M, Navas R, Gorgoglione A. Impacts of irrigation development on water quality in the San Salvador watershed (Part 1): Assessment of current nutrient delivery and transport using SWAT. Agrocienza Uruguay [Internet]. 2023 [cited dd mmm yyyy];27(NE1):e1198. Doi: 10.31285/AGRO.27.1198.



de nutrientes y permite caracterizar los procesos de exportación y transporte de nutrientes en la cuenca. La magnitud del escurrimiento afecta el balance de nutrientes. En condiciones de caudales altos las fuentes difusas predominan, mientras que en caudales bajos las cargas puntuales y las excreciones directas del ganado a cursos de agua son las principales fuentes. Los resultados de este trabajo contribuyen al diseño de estrategias para alcanzar una intensificación agrícola sostenible. También se documenta una nueva herramienta de modelación que queda disponible y puede utilizarse en estudios posteriores.

**Palabras clave:** agricultura sostenible, calidad de agua, SWAT

## Resumo

O cenário de desenvolvimento da agricultura resulta em mudanças no uso e gestão do solo e impacta a disponibilidade e qualidade da água. É fundamental projetar práticas de conservação e boas práticas agrícolas que atendam ao paradigma da intensificação agrícola sustentável. O objetivo deste trabalho foi compreender e caracterizar os processos-chave que afetam a hidrologia, a exportação e transporte de nutrientes, e quantificar os impactos na bacia do rio San Salvador. O modelo Soil & Water Assessment Tool (SWAT) foi implementado, a quantidade de água foi calibrada e a qualidade de água foi ajustada utilizando técnicas de calibração suave. O modelo reproduz adequadamente a quantidade de água e o balanço de nutrientes na bacia, permitindo caracterizar os processos de exportação e transporte de nutrientes na bacia. A magnitude do escoamento afeta o balanço de nutrientes. Com escoamento elevado, fontes difusas de nutrientes são mais significativas, enquanto em baixos níveis de escoamento, fontes pontuais e excrementos vacunos que escoam direto aos canais de drenagem prevalecem. Os resultados deste trabalho contribuem para o desenvolvimento de estratégias para uma intensificação agrícola sustentável. Também se descreve uma nova ferramenta de modelagem que fica disponível e pode ser usada em futuros trabalhos.

**Palavras-chave:** agricultura sustentável, qualidade de água, SWAT

## 1. Introduction

Intensive agricultural activities are one of the primary non-point sources of pollution that menace the quality of water bodies and the ecosystem's health<sup>(1)</sup>. Hence, sustainable land management and conservation practices have been increasingly implemented to reduce such types of pollution. For instance, one widely used conservation practice is riparian buffer zones<sup>(2)</sup>. Previous studies have demonstrated the positive effects of riparian buffer zones on water quality at the local field level<sup>(3)</sup>. However, such an effect should be evaluated at a watershed scale to aid river basin management programs. Therefore, hydrologic and water quality models at a basin scale are valuable tools for this purpose<sup>(4-5)</sup>. For decades, they have been used to assess stream flow and non-point source pollution along with the impacts (short- and long-term) of alternative management practices<sup>(6-7)</sup>. They are also valuable for determining the feasibility of water quality objectives at different budget levels, prioritizing sub-basins for watershed plan implementation, and identifying optimal conservation measures<sup>(8)</sup>.

In the scientific literature, there are several types of models based on physical hypotheses that simulate precipitation-runoff and pollutant delivery and transport processes. Lumped models consider the watershed as a single unit, averaging the spatial features related to the model response<sup>(9)</sup>.

Distributed models divide the catchment into elementary units, such as grid cells, and flows are routed from one cell to another as water drains through the basin. This allows the representation of watershed heterogeneity. The grid resolution is usually chosen to be of the appropriate size to represent the spatial variation of the main water quantity and quality processes. There are also semi-distributed models, which discretize the watershed into homogeneous sub-areas or sub-basins depending on the topography, the physical characteristics of the basin or the drainage area. Infiltration or precipitation parameters are treated as homogeneous within each sub-basin<sup>(10)</sup>. The Soil & Water Assessment Tool (SWAT)<sup>(11)</sup> model is one of the most widely adopted semi-distributed models in Uruguay<sup>(12-17)</sup>. It can generate precise results in the simulation of precipitation-runoff processes and pollutant delivery and transport.

A crucial aspect of modeling is understanding the key characteristics and processes of the watershed under study (water, sediment, nutrient, and carbon budgets)<sup>(18)</sup>. Although there is no universal method for calibrating and validating models, the use of soft data and various model performance criteria is increasingly recommended to ensure that models capture the main hydrologic and water quality processes<sup>(18-19)</sup>. Hard data are long-term, measured time series, while soft data are information about



specific processes that may not be directly measured, such as an average annual estimate<sup>(18)</sup>. Studies show the importance of constraining model parameters to obtain reasonable crop yields and water balances and to simulate realistic scenarios with different management practices<sup>(19)</sup>.

This study considered the San Salvador watershed, an agricultural basin in Uruguay. This basin is representative of the agricultural expansion process of the country<sup>(20)</sup> and now has the potential to intensify its production through supplementary irrigation<sup>(21-22)</sup>. The irrigation development changes land use and management and affects the water quality and quantity of the San Salvador River. In this investigation, the specific focus is on nutrients and sediments; however, pollutants encompass a broader range, including fertilizers, herbicides, insecticides, chemicals, sediments and metals. Understanding the fundamental processes affecting the delivery, transport, and transformation of nutrient and sediment and quantifying the impacts at the watershed scale are critical to evaluate and suggest the best management practices consistent with sustainable agricultural intensification.

Based on these considerations, the main objective of this study is to implement a SWAT model able to represent the stream flow and pollutant (nutrient and sediment) delivery and transport for the San Salvador watershed. This model will support sustainable land use strategies in a scenario of irrigation development. The specific objective is four-fold: i) to evaluate the applicability of the SWAT model in a data-scarce region based on well-known model performance indicators; ii) to reproduce spatially distributed flows and assess the water balance at the sub-basin level; iii) to simulate spatially distributed pollutant delivery and transport; iv) to let the model available to enable further studies and scenario modeling.

This study represents the first part of a master's thesis with the goal of constructing a modeling tool to support sustainable land use and planning in an agriculture irrigation development scenario. The scenario implementation and analysis were reported in the paper "Impacts of irrigation development on water quality in the San Salvador watershed (Part 2): Implementation of scenarios in SWAT"<sup>(23)</sup>.

## 2. Materials and methods

### 2.1 Study area

In this study, the watershed of the San Salvador River in the department of Soriano, Uruguay, is considered (Figure 1). The main river flows

northwesterly until it joins the Uruguay River. The watershed has an extension of 2,413 km<sup>2</sup> and an average slope of 2.3%. The city of Dolores is the main city in the watershed. It has 19,135 inhabitants<sup>(24)</sup> and is located at the watershed outlet. The average annual temperature and total precipitation during the period 1961-1990 are 17.5 °C and 1100 mm, respectively<sup>(25)</sup>.

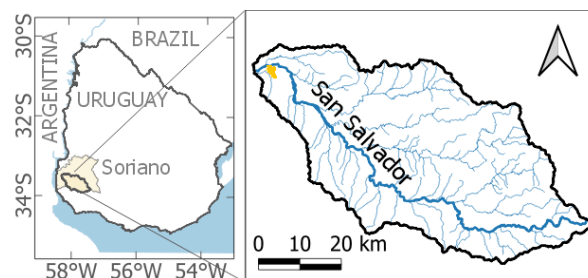


Figure 1. Location of the San Salvador watershed (Soriano department, Uruguay). Coordinate Reference System: World Geodetic System 1984 (WGS84)

Between 1990 and 2018, a remarkable change in land use was registered in the San Salvador basin (Table 1 and Figure 2)<sup>(20)</sup>: cropland increased from 953 to 1,495 km<sup>2</sup> (57%), grassland decreased from 1,358 to 749 km<sup>2</sup> (45%), and production forest increased from 12 to 78 km<sup>2</sup> (570%). Land management also changed: in 1990, cropping with grazing combined with livestock and till practices prevailed, while in 2018, continuous cropping, no-till, and transgenic crops prevailed<sup>(26)</sup>. In 1990, winter crops in Soriano were three times larger than summer crops, and the main crops were winter wheat, barley, and sunflower<sup>(27)</sup>. However, in 2018, summer crops were twice as long as winter crops, and soybeans were the main crop<sup>(28)</sup>.

### 2.2 Data availability

SWAT requires specific data about weather, soil properties, topography, vegetation, and land management practices of the watershed<sup>(30)</sup>. An overview of the input data used in this study is provided in Table S1 in the Supplementary Materials. Geospatial input data include digital elevation model<sup>(31)</sup> (DEM) (Figure 3), 1990 and 2018 Land Use / Land Cover (LULC) maps<sup>(20)(29)</sup> (Figure 2), and soil map<sup>(32)</sup> (scale 1:40,000).

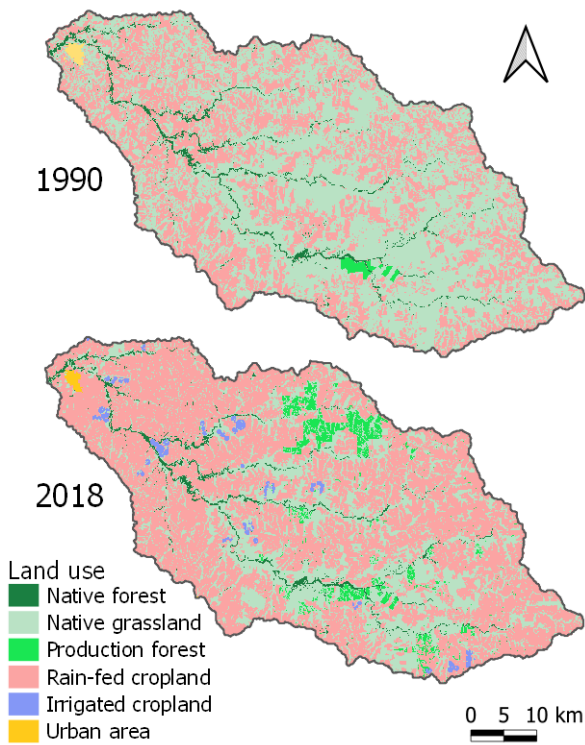


Figure 2. Land use maps of the San Salvador watershed: in 1990 (on top) and 2018 (bottom). Maps were simplified by Hastings and others<sup>(20)</sup> and Petraglia and others<sup>(29)</sup>, respectively

Table 1. Area (km<sup>2</sup>) of land use (LU) classes in 1990 and 2018 in the San Salvador watershed. LU classes were simplified by Hastings and others<sup>(20)</sup> and Petraglia and others<sup>(29)</sup>, respectively

Class	LU 1990	%	LU 2018	%
Native grassland	1,358	56.9%	749	31.0%
Rain-fed cropland	953	39.8%	1495	62.0%
Native forest	57	2.4%	57	2.4%
Production forest	12	0.5%	78	3.2%
Urban area	10	0.4%	5	0.2%
Irrigated cropland	---	---	28	1.2%

According to the soil map, there are 37 units in the watershed. The predominant soil type is Vertic Argiudoll (90%), which has high natural fertility and agricultural productivity in Uruguay. At SWAT, soil data are divided into physical and chemical characteristics. For the physical characteristics, the data are sourced from soil profiles linked to each map unit<sup>(32)</sup> or computed using the Soil-Plant-Air-Water (SPAW) model<sup>(35)</sup>. The soil units were classified into hydrological groups (HG) using the methodology proposed in the documentation of SWAT<sup>(30)</sup> and validated with the work of Durán<sup>(36)</sup> with very good agreement. The results show that HG classes D and C are predominant in the basin, with 70% and 21%, respectively (Figure 4). Regarding chemical characteristics, the contents of total nitrogen (TN) and Bray I phosphorus are reported for the soil profiles associated with each map unit. Nitrogen content was assumed to be 98% organic and 2% inorganic<sup>(37)</sup>; total phosphorus (TP) content was determined by a regression based on clay content and assumed to be 50% organic and 50% inorganic<sup>(38)</sup>.

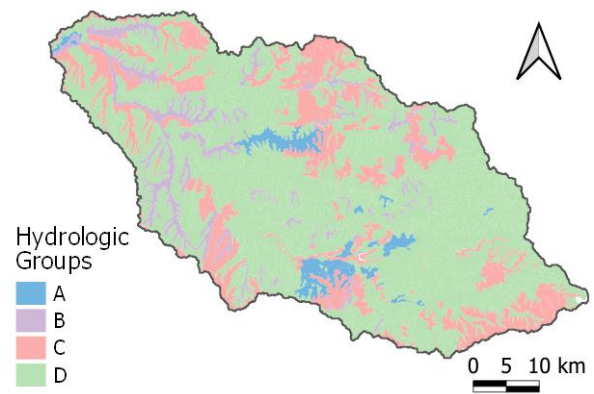


Figure 4. Hydrologic groups estimated from Soil Map, esc.: 1:40.000<sup>(32)</sup>

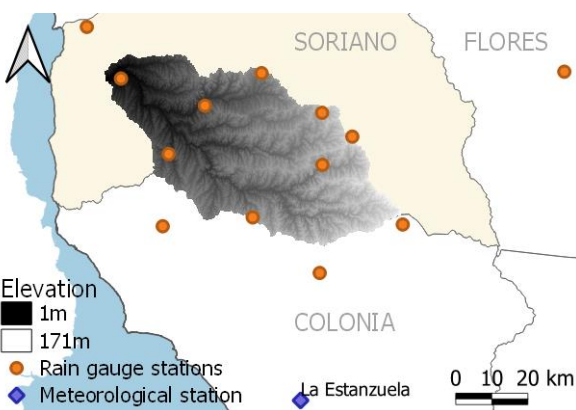


Figure 3. Elevation digital model<sup>(31)</sup>, rain gauge stations<sup>(33)</sup>, and meteorological station<sup>(34)</sup>

Daily precipitation data from 1987 to 2021 are from 14 rain gauging stations<sup>(25)(33)</sup> in and around the watershed. Daily weather data (minimum and maximum air temperature, wind speed, relative humidity, and solar radiation) from 1987 to 2021 were recorded from the nearest meteorological station<sup>(34)</sup>. Figure 3 shows the location of the meteorological station and rain gauges. As the weather conditions within each sub-basin are homogeneous, the daily mean areal precipitation was calculated for each sub-basin using the inverse distance weighting method<sup>(39)</sup> and then employed as input data for SWAT.

In the watershed, there is a single gauging station situated at Paso Ramos (outlet of sub-basin 12, Figure 5) (58° 09' 49" W, 33° 33' 15" S), which pertain



to the National Water Directorate of the Ministry of Environment (DINAGUA-MA)<sup>(40)</sup>. Water levels at this station were manually recorded from 1985 to 2006, and discharges were computed using a rating curve. Although data is available until 2006, according to DINAGUA, only measurements up to 2000 are considered reliable. Rating curves are utilized to compute flow time series from water levels. These curves are derived empirically through field measurements and can introduce notable uncertainties that impact the calibration procedure of the hydrological model<sup>(41)</sup>. According to the station data quality analysis<sup>(42)</sup>, the error is 33% for low flows (1.4 - 6.8 m<sup>3</sup>/s) and 20% for medium flows (6.8 - 86 m<sup>3</sup>/s). The peak and low flows (86 - 2000 m<sup>3</sup>/s, and 0 - 1.4 m<sup>3</sup>/s, respectively) are ranges that were not recorded, so they were extrapolated from the rating curve and are subject to bigger uncertainties.

There are ten water quality stations in the watershed, seven along the San Salvador River that have been in operation since 2014, and four stations on tributaries that have been in operation since 2019 (Figure 5). The station designated SS50 is in Paso Ramos, where the stream flow station is. Monitoring has been conducted once every two months by State Sanitary Works Administration (OSE) and National Directorate for Quality and Environmental Assessment of the Ministry of Environment (DINACEA-MA) since 2016 and at a lower frequency since 2014. In addition, five campaigns were carried out in 2020-2021 as part of the INNOVAGRO project<sup>(39)</sup>. For this study, of the 44 parameters analyzed regularly, TN, TP, and total suspended solids (TSS) are considered. Table S8 shows the number of samples and the mean, minimum and maximum values measured for TN, TP, and SST.

Point sources of pollution are domestic sewage in the city of Dolores and intensive livestock production (fattening farms and dairies). Dolores has a total population of 19,135 and discharges its domestic wastewater directly into the San Salvador River. Nutrient loads from domestic sewage are estimated using population size and bibliographic coefficients<sup>(43)</sup>. Nutrient load from fattening farms and dairies is calculated using the estimated number of cattle in each sub-basin<sup>(44)</sup> and the calculations proposed by DINAMA<sup>(45)</sup>. According to the National Livestock Information System and the Livestock Comptroller's Division of the Ministry of Livestock, Agriculture, and Fisheries (SNIG and DICOSE-MGAP)<sup>(44)</sup>, the stock of cattle in fattening farms and dairies in the study area in 2018 was 12,595 and 6,646 cattle units, respectively.

Another direct source of nutrients is the free access of cattle to watercourses. In Uruguay, this is a common management practice related to grazing on native grasslands and seeded pastures<sup>(46)</sup>. In the absence of information on the proportion of the area where this practice is applied and the proportion of manure directly deposited by cattle, it is assumed that 5% of cattle manure directly enters watercourses. According to SNIG and DICOSE<sup>(44)</sup>, the stock of cattle grazing native grasslands and seeded pastures in the study area in 2018 was 58,972 and 3,905 cattle units, respectively.

SWAT includes scheduled management practices such as crop rotation, planting, harvesting, irrigation, fertilization, and tillage. Crop rotations for 1990 are based on information from the 1990 General Census of Agriculture, where two rotations of cropping with grazing combined with livestock are considered (Table S2). For 2018, rotations are based on interviews with technicians of the General Directorate of Natural Resources of the MGAP (DGRN-MGAP), where four rotations of continuous cropping and one rotation of cropping with grazing combined with livestock are considered (Table S3). Additionally, Table S4 shows the cropping cycle and annual fertilizer rates.

The reference data for erosion rates were provided by DGRN and correspond to the annual averages obtained for Uruguay during 2000-2020 using the Revised Universal Soil Loss Equation (RUSLE)<sup>(47)</sup>.

### 2.3 Model description and set up

The Soil & Water Assessment Tool (SWAT) is a model for predicting the effects of land use, land management, and climate change on water resources<sup>(11)</sup>. It is widely used to assess nutrient loading and soil erosion in agricultural basins. The model allows the simulation of various biophysical processes such as runoff, infiltration, water storage, routing, crop yield, sediment transport, and nutrient cycling. The version of the model used is SWAT 2012, including SWAT Editor (2020 Revision 681) and QSWAT interface (version 1.9), available for QGIS (version 2.6.1).

Geospatial data were processed using QGIS (version 3.16.11), converting maps to raster format and projecting to the WGS 84 / UTM Zone 21S coordinate reference system. Thirteen sub-basins were delineated using the QSWAT interface, considering that outlets coincide with hydrometric and water quality stations (Figure 5). The sub-basins range from 47 to 341 km<sup>2</sup>; sub-basins 4 and 11 were also delineated to subdivide a large one.

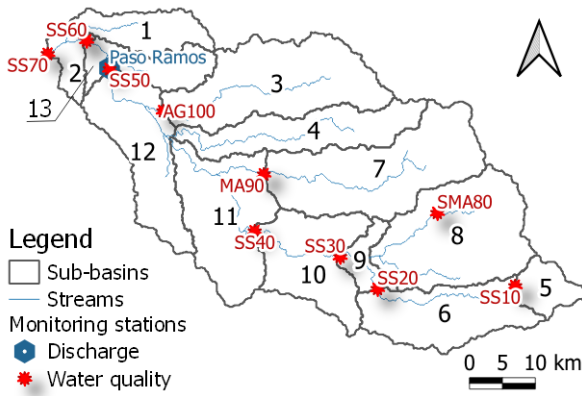


Figure 5. Monitoring stations (DINAGUA and DINACEA-MA) and SWAT sub-basins

Due to the lack of accompanying observations on stream flow (1988-2006) and water quality (2014 to present), two models based on LULC and crop rotations from 1990 and 2018 were implemented; the first model was used to calibrate stream flow and the second model was used to verify water quality. The Split Land Use tool of SWAT was used to divide the rain-fed cropland, considering the main crop rotations and their relative extension (Table S2 and Table S3): two rotations for 1990 and five for 2018.

Hydrological response units (HRUs) are the basic computational unit of the model, and the number of HRUs depends on the heterogeneity of the input maps and the number of sub-basins. Given the computational limitations, it was necessary to reduce the initial number of HRUs. SWAT allows the application of filters based on the proportion of land use, soil, and slope to reduce the number of HRUs, but simulated water quality is sensitive to information loss<sup>(48)</sup>. Following the recommendations of Her and others<sup>(48)</sup>, we simplified the input maps to reduce the number of HRUs rather than applying filters. In this sense, we (1) reduced the original resolution of the maps (Table S1) resulting in a pixel size of 120×120 m; (2) simplified the LULC maps, eliminating two minor classes (water 0.15% and bare soil 0.02%), noted that water bodies in SWAT are modeled by channels (streams) and reservoirs. Note that the number of HRUs with agricultural land use increased due to the representation of crop rotations, but the split allows for a detailed spatial distribution of the main crop rotations. (3) Simplified the soil map, considering a maximum of 5 soil classes for each land use in each sub-basin, and reassigning minority classes according to hydrologic group and texture. These changes reduced the number of HRUs to 487 and 1354 for LULC 1990 and 2018, respectively.

The plant growth module of SWAT simulates biomass accumulation, nutrient uptake, and yield at harvest<sup>(30)</sup>.

The delivery of sediment and nutrients from the soil to water results from weathering acting on land-forms<sup>(30)</sup>. SWAT uses the Modified Universal Soil Loss Equation (MUSLE)<sup>(49)</sup> to determine sediment yield daily:

$$sed = 11.8 \times (Q_{surf} \times q_{peak} \times area_{HRU})^{0.56} \times K_{USLE} \times C_{USLE} \times P_{USLE} \times LS_{USLE}$$

Where *sed* is the sediment yield on a given day (Mg/ha/day);  $Q_{surf}$  is the surface runoff volume (mm);  $q_{peak}$  is the peak runoff rate (m<sup>3</sup>/s);  $area_{HRU}$  is the area of HRU (ha);  $K_{USLE}$  is the soil erodibility determined from soil data;  $C_{USLE}$  is the cover and management factor obtained from local research (Table 2);  $P_{USLE}$  is the support practice factor and is set equal to 1;  $LS_{USLE}$  is the topographic factor and is obtained from the slope length and average slope of the sub-basin (both calculated from DEM)<sup>(30)</sup>. RUSLE predicts the mean annual erosion rate and involves the consideration of a sediment delivery ratio for the computation of sediment yield<sup>(50)</sup>. On the other hand, MUSLE substitutes the rainfall energy factor with a runoff factor, allowing the equation to be applied to individual storm events for the calculation of sediment yield<sup>(30)</sup>.

Table 2. USLE cover and management factor<sup>(51)</sup>

Land use	C <sub>USLE</sub>
Native grassland	0.02
Production forest	0.006
Cropland with pastures, no till	0.02
Cropland, no till	0.036

SWAT simulates the transformation and movement of nitrogen and phosphorus in various organic and inorganic pools<sup>(30)</sup>. Soil N cycling has five different organic and inorganic pools; N transformation includes mineralization, decomposition and immobilization, nitrification, denitrification, and ammonia volatilization. Other N processes include plant uptake, biological N fixation, and NO<sub>3</sub>-N movement in the water. The P cycle in the soil has six different organic and inorganic pools; the transformation of P in soil includes mineralization, decomposition, immobilization, and other processes such as plant uptake. Nitrates and soluble P are removed from the topsoil layer by surface and subsurface runoff. The amount of organic N and P transported with sediments is a function of organic N and P in the topsoil layer and sediment yield. In this study, nutrient



yields are the total N or P loading delivered from HRU to stream.

SWAT can model in-stream processes that affect nutrient and sediment transformation and transport using QUAL2E<sup>(52)</sup> algorithms. The data used for in-stream water quality correspond to sediment and nutrient yields from HRUs and point sources.

## 2.4 Hard and soft model calibration

The calibration approach included hard and soft data<sup>(18)</sup>. Discharge data from the Paso Ramos gauging station were used for discharge calibration and validation. Due to the low sampling frequency (every three months), water quality was soft-calibrated. Crop yields, sediment yields, and nutrient cycling were also soft-calibrated using local data.

### 2.4.1 Crop soft-calibration

In SWAT, the processes involving crops, water, and nutrients are interconnected. The initial stage of model calibration focused on a soft calibration of crop growth. This calibration approach results in improved water and nutrient budgets compared to traditional approaches (without crop calibration)<sup>(53)</sup>.

The model was soft-calibrated by comparing the annual average of simulated to observed (Uruguayan Federation of Crea Groups, FUCREA and Uruguay United Irrigators Association, RUU) crop yields for soybeans, corn, winter wheat, and barley. For native grasslands, native forests, and production forests, biomass was compared using available data (Table S1).

### 2.4.2 Flow calibration and validation

The steps to calibrate the flow discharge were: (1) performing a sensitivity analysis using extended Fourier amplitude sensitivity testing (eFAST)<sup>(54)</sup>, after which the parameters with the highest sensitivity index for calibration were selected (the indices are calculated as the ratio of each partial variance to variance of the model output); (2) performing several calibration tests, including two methods for calculating evapotranspiration (Penman-Monteith and Hargreaves), two methods for stream flow routing (variable storage and Muskingum), and two algorithms for calibration (Sequential Uncertainty Fitting, SUFI2<sup>(55)</sup>, and Particle Swarm Optimization, PSO<sup>(56)</sup>), with one option selected after the tests; (3) based on the initial calibration results, the base flow was manually adjusted varying the groundwater parameters; (4) with the groundwater parameters fixed, the surface runoff parameters were calibrated; (5) the flow validation was performed.

The parameters included in eFAST analysis were selected based on the literature<sup>(57-58)</sup>. A brief description of each parameter, the process in which it is involved, the default values in the model, and the range of values considered are shown in Table S7. In addition, some parameters were divided into two groups according to the land use: (A) native grassland, rainfed agriculture, and rainfed agriculture with pasture; (B) production forest and native forest.

Discharge was calibrated for 1990-1998 and validated for 1999-2000 with a daily time step, and a three-year warm-up period 1987-1989 was used to stabilize the model's initial conditions. The SWATrunR package<sup>(59)</sup> in R was used to perform sensitivity analysis, calibration, and validation. Nash-Sutcliffe efficiency (NSE)<sup>(60)</sup> was used as the objective function for model simulation optimization. Additionally, percent bias (PBIAS) and Kling-Gupta efficiency (KGE)<sup>(61)</sup> were calculated to evaluate model performance. NSE determines the relative magnitude of residual variance compared to measured data variance and has its optimum at 1<sup>(62)</sup>. PBIAS indicates the average tendency of the simulated data to be larger or smaller than the observed data; its optimal value is 0, and positive or negative values of PBIAS indicate bias as underestimation or overestimation, respectively<sup>(62)</sup>. Stream flow simulation can be considered satisfactory if NSE > 0.50 and PBIAS is in the range [-15%, 25%]<sup>(62)</sup>. KGE is a combination of the correlation coefficient, bias ratio, and variability ratio that allows optimization based on multiple criteria; its optimum is 1, and values in the range [-0.41, 1] can be considered satisfactory performance<sup>(63)</sup>.

### 2.4.3 Sediment yield verification

For verification, the 2000-2020 annual average of simulated sediment yield was compared to the erosion rates provided by DGRN.

### 2.4.4 Phosphorus and nitrogen yields verification

Nutrient yields were soft-calibrated by comparing the annual average of simulated values with values from a literature review commonly used in Uruguay<sup>(64)</sup>. Additionally, the P index<sup>(65)</sup> soft data was recently estimated in Uruguay to assess the risk of P delivery from agricultural lands to surface waters. The values of P index were also compared to annual average of simulated nutrient yields.

### 2.4.5 Water quality verification

A global sensitivity analysis was conducted using eFAST, and the most sensitive parameters were adjusted. The goal of this soft-calibration was to align

the average observed TN and TP values with those from a subset of simulations. To make a more accurate comparison, as the sampling is once every two months but simulations are daily, a subset of twenty-one days centered around the sampling day was employed instead of considering the entire set of simulations. For this analysis, the SWATrunR package<sup>(49)</sup> in R was employed, utilizing the PSO algorithm to enhance the optimization of water quality simulations.

## 2.5 Analysis of nutrient delivery and transport

The approach of duration curve from US Environmental Protection Agency (US EPA)<sup>(66)</sup> was used to analyze nutrient delivery and transport in the San Salvador watershed. This approach allows the characterization of water quality data under different flow regimes. It can be used as a diagnostic tool to determine the magnitude and frequency of exceedances of water quality standards under all flow regimes.

The discharge duration curve relates daily discharge values to the percentage of the time those values were equaled or exceeded. Five hydrologic condition zones are distinguished: high flows (0-10%), moist conditions (10-40%), mid-range flows (40-60%), dry conditions (60-90%), and low flows (90-100%).

In this study, load-duration curves were generated by multiplying simulated flow by water quality concentrations. Analysis was performed for TN and TP. The curve compares three loads: observed, simulated, and targeted<sup>(67)</sup> during 2014-2021 in Paso Ramos (sub-basin 12). Targeted load refers to the allowable, considering the concentration levels specified in the local water quality guidelines<sup>(67)</sup>. Further, a source-duration curve was created to determine the contributions from the different sources to the nutrient load, using daily cumulative nutrient yields and point source loading up to Paso Ramos. It is worth noting that the observed load was calculated with simulated flow data since the observed flow is unavailable for this period. As previously discussed (Section 2.2), the zones of high and low flow have greater uncertainty; this uncertainty extends to the load curves within these specific zones.

A fundamental premise of this approach is the correlation of nutrient sources and water quality with flow conditions. These curves link water quality impairments to major sources. However, they do not account for processes such as sedimentation, plant uptake, or chemical transformations.

## 3. Results and discussion

### 3.1 Hard and soft model calibration

#### 3.1.1 Crop soft-calibration

Soft-calibrated parameters and fitted values are summarised in Table S5 and Table S6. Table 3 shows the average annual yield and biomass for observed and simulated data. After stream flow calibration, biomass and yield differed slightly; the results presented are the final values. However, this was the first step in calibrating the model because plant growth, especially perennial plants, was poorly represented. Since the difference between simulated and observed annual averages was less than 20%, we assumed good agreement between simulated and observed data.

Table 3. Crop yield and plant biomass soft-calibration results 2010–2021

Plant	Observed	Simulated	$\Delta$ (%)
<b>Yields (kg/ha)</b>			
Corn 1 <sup>st</sup>	6,133	6,938	13%
Corn 1 <sup>st</sup> irrigated	11,060	11,591	5%
Soybean 1 <sup>st</sup>	2,625	2,794	6%
Soybean 2 <sup>nd</sup>	2,159	2,552	18%
Soybean 1 <sup>st</sup> irrigated	4,052	3,814	-6%
Winter Wheat	3,805	3,728	-2%
Barley	3,737	3,395	-9%
<b>Biomass (kg/ha)</b>			
Native grasses	5,031	4,175	-17%
Pasture	6,600	6,179	-6%
Native forest	122,000	103,000	-16%
Production forest	240,000	228,000	-5%

#### 3.1.2 Flow calibration and validation

Five steps are involved in the flow calibration and validation process (section 2.3). The first step was the sensitivity analysis performed using eFAST<sup>(57-58)</sup>. According to the analysis, the most sensitive parameter was CN2(A), with a sensitivity index of 0.55, while the index for the other parameters was less than 0.06 (Figure 6). The ten parameters with the highest sensitivity were considered for flow calibration: CN2(A), ALPHA\_BF, CH\_N2, ESCO\_A, CH\_L2, GWQMN, SOL\_AWC, SLSUBBSN, OV\_N\_A, CH\_S2.

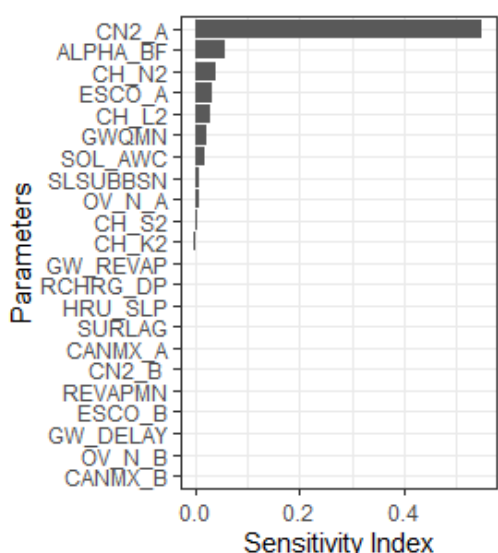


Figure 6. Results of the flow sensitivity analysis

Some calibration tests were performed with two methods for evapotranspiration calculation, two methods for flow routing, and two algorithms for calibration. The configurations tested did not significantly improve the results as NS, PBIAS, and KGE that varied from 0.51 to 0.55, -14% to -19%, and 0.47 to 0.52, respectively. The selected configuration includes the Penman-Monteith and Variable Storage methods for calculating evapotranspiration and flow routing, respectively. The PSO algorithm was chosen because it has the highest NS and acceptable PBIAS and KGE. Based on the initial calibration results, groundwater flow was adjusted manually by varying the parameters ALPHA\_BF and GW\_DELAY, with GW\_DELAY included because it appeared sensitive. Once fixed the groundwater parameters, the surface runoff was automatically calibrated by the PSO algorithm; the resulting parameters are listed in Table 5. Afterward, the flow validation was performed.

Table 4 shows the performance results of the calibration and validation, and Figure 7 shows the flow duration curves, simulated and observed (1990-2000). According to Moriasi and others<sup>(62)</sup>, the performance of the calibration was satisfactory. In the validation period, NSE decreased to an unsatisfactory level, and KGE and PBIAS remained satisfactory. Therefore, the hydrologic submodel performance is considered adequate, according to the available data. The guidelines for quantification of accuracy<sup>(62)</sup> suggest a comparison metric for the simulations. However, it is important to note that the guidelines do not consider the uncertainty of climate forcing<sup>(68)</sup> and/or hypothetical scenarios<sup>(69)</sup>. To account and adjust for different sources of errors in the

hydrological model output, error models could be used<sup>(70)</sup>.

### 3.1.3 Sediment yield verification

Table 6 compares the reference erosion rate for each land use with the average annual sediment yield for 2000-2020. The simulated averages are of the same order of magnitude as the reference values. Moreover, they are generally within the reference range, except for agriculture, where the simulated value is slightly higher. Additionally, Table S9 presents sediment yield mean values (2014-2021) per sub-basin and land use category.

Table 4. The SWAT model performance metrics during the calibration and validation of daily stream flow

	NS	KGE	PBIAS
Calibration	0.55	0.47	-9
Validation	0.37	0.5	-12.5

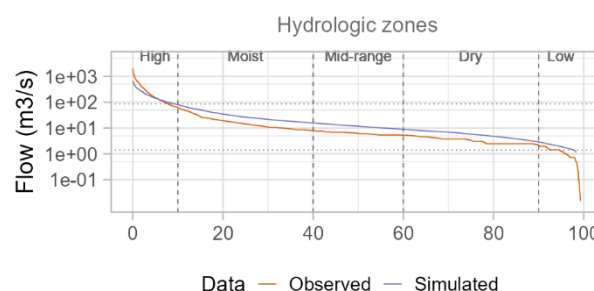


Figure 7. Flow duration curves, simulated and observed, 1990-2000

Table 5. The most sensitive parameters and the adjusted values after flow calibration

Parameter	Table	Unit	Change	Final
CN2 (A)	mgt	---	Relative	8.5%
ALPHA_BF	gw	1/day	Absolute	0.85
CH_N2	rte	---	Absolute	0.03
ESCO	hru	---	Absolute	0.87
CH_L2	rte	km	Relative	-13.1%
GW_DELAY	gw	days	Absolute	70.37
SOL_AWC	sol	mmH <sub>2</sub> O/ mm soil	Relative	64.0%
SLSUBBSN	hru	m	Relative	75.1%
OV_N	hru	---	Relative	-22.2%
CH_S2	rte	m/m	Relative	41.4%

Table 6. Mean sediment yield simulated with SWAT and erosion rates reported by DGRN, standard deviations are enclosed within parenthesis, 2010-2020

Land use	Erosion rate DGRN (Mg/ha/yr)	Sediment yield SWAT (Mg/ha/yr)
Irrigated cropland	---	4.29 (2.55)
Rainfed cropland	2.74 (1.57)	4.34 (2.56)
Rainfed cropland with pastures	---	2.13 (1.35)
Production forest	0.89 (0.5)	0.43 (0.32)
Native forest	0.99 (0.86)	0.19 (0.14)
Native grassland	1.86 (1.49)	2.49 (1.42)

### 3.1.4 Phosphorus and nitrogen yield verification

Table 7 presents the average annual yields of TN and TP in 2014-2021, along with corresponding bibliographic references<sup>(64)</sup> for each land use category. Additionally, Table S9 presents TN and TP mean values per sub-basin and land use category. The simulated averages are in the same range as the reference values, except for production and native forests, where the simulations show lower TN yields. Additionally, the P-index (2014-2018) holds a slightly higher value compared to the simulated average TP. However, it is worth noting that the P-index was calculated over different periods and for the entire Uruguay.

Table 7. Simulated (2014-2021) mean and standard deviation of yields from Total Nitrogen (NT) and Total Phosphorus (kg/ha/year), soft data from the scientific literature (min.-max.)<sup>(64)</sup>, and P index<sup>(65)</sup>

Land use	Bibliography	Sim. mean	Sim. sd	
<b>NT (kg/ha/yr)</b>				
Irrigated cropland	---	17.25	8.75	
Rain-fed cropland	15.4 (3.2-47.7)	12.96	6.47	
Cropland with grazing	7.0 (1.5-21.1)	9.78	3.82	
Production forest	1.9 (0.8-3.7)	0.25	0.14	
Native forest	0.4	0.02	0.01	
Native grassland	1.3 (0.4-3.3)	2.26	0.93	
<b>PT (kg/ha/yr)</b>				<b>P<sub>Index</sub></b>
Irrigated cropland	---	2.93	1.34	
Rain-fed cropland	4.11 (0.32-16.71)	2.54	1.15	3.46
Cropland with grazing	1.79 (0.15-7.06)	2.7	0.98	
Production forest	0.29 (0.03-0.65)	0.18	0.11	1.79
Native forest	0.01	0.08	0.05	
Native grassland	0.24 (0.03-0.62)	1.14	0.48	2.35

### 3.1.5 Water quality verification

Table 8 presents the most sensitive parameters and the adjusted values after water quality calibration. Figure 8 shows box plots comparing the simulated and observed concentrations of TN and TP. The simulated values upstream (small sub-basin extension) overestimated the concentrations of TN and TP. However, the concentrations at stations SS40 to SS70 show good agreement (see location of stations in Figure 5).

Table 8. The most sensitive parameters and the adjusted values after water quality calibration

Parameter	Table	Unit	Final	Description
SPCON	rte	---	0.000 2	Linear parameter for calculating the maximum amount of sediment that can be reentrained during channel sediment routing.
ERORGP	hru	---	0.638	Organic P enrichment ratio for loading with sediment.
P_UPDIS	bsn	---	13.34 4	Phosphorus uptake distribution parameter.
NPERCO	bsn	---	0.000 1335	Nitrogen percolation coefficient.
BIOMIX	mgt	---	0.2	Biological mixing efficiency.
ERORGN	hru	---	3.267	Organic N enrichment ratio for loading with sediment.

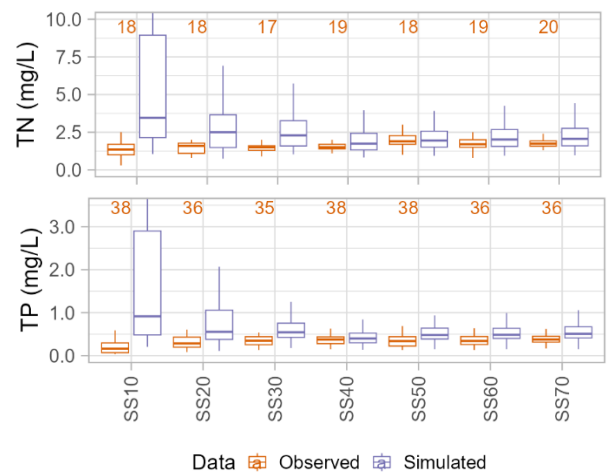


Figure 8. Simulated and observed concentrations of Total Nitrogen (NT) and Total Phosphorus (TP) (mg/L), 2014-2021. The orange numbers represent the number of observations at each monitoring station



### 3.2 Analysis of nutrient delivery and transport

Load-duration curves for the 2014-2021 period in Paso Ramos (sub-basin 12) were generated for TN and TP (Figure 9 and Figure 10). Overall, there is a good agreement between observed and simulated nutrient loads (Figure 9 and Figure 10, Part C). However, under dry and low-flow conditions, the simulation overestimates the loads. As shown, the pattern of nutrient impairment occurs under all flow conditions as the observed and simulated nutrient loads exceed the target loads<sup>(67)</sup>. It is worth noting that the load results in zones of high and low flow exhibit higher uncertainty, as discussed in Section 2.5.

The source-duration curves (Figure 9 and Figure 10) (Part A) and their relative contribution by source and hydrologic zone (Part B) showed that, between mid-range and low flows, the main loads come from direct livestock excreta into water bodies and point sources from feedlots and dairies. In addition, under wet and high-flow conditions, diffuse sources associated with land use mainly affect water quality.

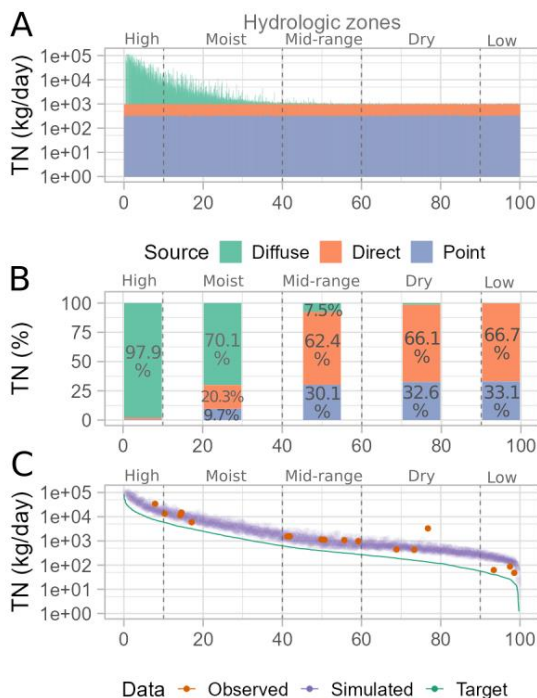


Figure 9. Total Nitrogen (TN) loads from 2014 to 2021 in Paso Ramos. (A) Load duration curve showing contributions from various sources; in this case, loads include cumulative yields from TN and point source loads in Paso Ramos. (B) Relative contribution of sources by hydrologic zone. (C) Load duration curves comparing observed and simulated data to the target curve

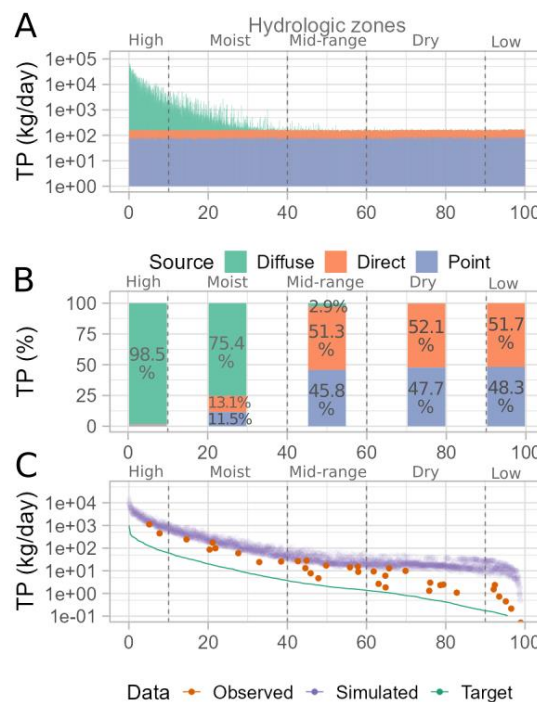


Figure 10. Total Phosphorus (TP) loads from 2014 to 2021 in Paso Ramos. (A) Load duration curve showing contributions from various sources; in this case, loads include cumulative yields from TP and point source loads in Paso Ramos. (B) Relative contribution of sources by hydrologic zone. (C) Load duration curves comparing observed and simulated data to the target

For moist to high-flow conditions, the major source is diffuse loading associated with land use. The nutrient diffuse contribution is about 98% and 73% for high and moist conditions, respectively. Within the diffuse loadings, the main contributors in order of importance are rain-fed agriculture, agriculture with grazing, and natural grassland with grazing. Table S12 shows the proportional contribution of each source type by hydrologic condition zones. Moreover, within Table S9, Table S10 and Table S11, the average contribution of each source type per sub-basin are presented.

For low to mid-range flow conditions, the major sources of nutrients are direct excretions from cattle to water bodies and point sources. The direct loading contribution is about 65% for TN and 51% for TP. Within the total direct load (TN and TP), the load from natural grassland is 1.7 times higher than from agriculture with grazing. In addition, the contribution from point sources is about 32% for TN and 47% for TP. Within point sources, the load from dairies is higher than from fattening farms, with a value of 1.8 times for TN and 2.4 times for TP.

During dry and low flow conditions, simulations showed an overestimation of TN and TP loads. In

the model, these input loads were not evaluated from measures but were calculated from the number of cattle, 84,849 cattle units<sup>(44)</sup> in the watershed in 2018. The amount of direct excretion of cattle into water bodies was an assumption based on the knowledge that this practice exists. Besides, wastewater discharges from fattening farms and dairies are assumed to be constant over time but may fluctuate with runoff because wastewater is typically stored in lagoons. Therefore, further research is needed to improve information on excreta input loads.

Considering all flow conditions, diffuse loading from cropland was the main source of nutrient loading (77% and 71% of total loading from TN and TP, respectively, during 2014-2021). However, the load-duration curve approach showed that diffuse loading explained nutrient impairment only 40% of the time during high and wet flow conditions. For low to mid-range flow conditions (the remaining 60% of the time), water quality can be explained primarily by the contribution of direct excretions from cattle to water bodies and point sources (dairies and fattening farms). This characterization of nutrient budgets indicates that: (1) nutrient balance impairment occurs under all flow conditions; (2) to achieve sustainable agricultural intensification a range of conservation measures and best management practices (BMPs) should be implemented. Diffuse sources pose a significant challenge because nutrients enter surface waters through various mechanisms (e.g., runoff, groundwater infiltration)<sup>(1)(11)(30)</sup>. BMPs<sup>(2)(4)(8)</sup> generally focus on source control (practices to reduce erosion) or delivery reduction (e.g. riparian buffers to intercept nutrients<sup>(3)</sup>). Direct loading control includes measures to prevent animal access to water bodies, restore banks, and prevent excess nutrients from entering the water. Point source control includes the treatment and management of wastewater from dairy and fattening farms<sup>(4)(8)</sup>.

#### 4. Conclusions

In this study, a model SWAT was implemented that can characterize water quantity and quality in the San Salvador watershed. The main results obtained with such a model can be summarized as follows:

Calibration and validation of stream flow were successfully performed (NSE=0.55 and 0.37, PBIAS= -9 and -12.5, KGE=0.47, 0.5, for calibration and validation, respectively). Biomass, crop, sediment, nitrogen and phosphorus yields, and water quality showed good agreement with local soft data. The evaluation by hard and soft calibration and with

available knowledge and data indicates that it is possible to fill the data shortage and build a reliable model.

The pattern of nutrient impairment occurs under all flow conditions as the observed and simulated nutrient loads exceed the target loads. Although diffuse loading from cropland was the primary source of nutrient loading (77% and 71% of total loading from TN and TP, respectively, during 2014-2021), the loading duration curve approach showed that this result was present in only 40% of the time during high and wet runoff conditions. For low to moderate runoff conditions (the remaining 60% of the time), water quality can be explained primarily by the contribution of direct excretions from cattle to water bodies and point sources (dairies and feed-lots).

It is important to emphasize that the model developed in this study SWAT is suitable to represent the crops and land management practices typical of South America and the resulting sediment and nutrient fluxes. In addition, it represents a useful tool to facilitate informed decisions in the development of strategies to mitigate pollution impacts on receiving waters.

#### Acknowledgements

This study is part of the master's thesis by Florencia Hastings from FAGRO-Udelar. It was partially supported by the National Research and Innovation Agency [grant numbers: POS\_NAC\_2020\_1\_164287 and FSA\_PI\_2018\_1\_148628].

We are sincerely grateful to the colleagues who contributed significantly to the modeling decisions with information and/or discussions; they represented the following institutions (in alphabetical order): Integrated Watershed Modeling Group (GMIC); Ministry of Livestock, Agriculture and Fisheries (MGAP); Ministry of Environment (MA); School of Agronomy, Universidad de la República (FAGRO-Udelar); School of Engineering, Universidad de la República (FING-Udelar), Uruguay United Irrigators Association (RUU).

#### Transparency of data

The model implemented in this work and the water quality data are freely available on the OSF platform: <https://osf.io/ytn9g/>



## Author contribution statement

HF: Methodology, software, validation, formal analysis, investigation, data curation, writing - original draft, visualization, funding acquisition.

PBM, NR and GA: Conceptualization, methodology, writing - review & editing, supervision, funding acquisition.

## References

- Ullrich A, Volk M. Application of the Soil and Water Assessment Tool (SWAT) to predict the impact of alternative management practices on water quality and quantity. *Agric Water Manag.* 2009;96(8):1207-17.
- United States Department of Agriculture, NRCService. Core4 conservation practices training guides: the common sense approach to natural resource conservation. Washington: USDA; 1999. 395p.
- Calvo C. Rol ecosistémico de la zona riparia en sistemas dulceacuícolas en un escenario de cambio global[doctoral's thesis]. Montevideo (UY): Universidad de la República, Facultad de Agronomía;2022.146p.
- Merriman KR, Gitau MW, Chaubey I. A tool for estimating best management practice effectiveness in Arkansas. *Appl Eng Agric.* 2009;25(2):199-213.
- White MJ, Arnold JG. Development of a simplistic vegetative filter strip model for sediment and nutrient retention at the field scale. *Hydrol Process.* 2009;23(11):1602-16.
- Osmond DL, Meals DW, Hoag DL, Arabi M, Luloff AE, Jennings GD, McFarland ML, Spooner J, Sharpley AN, Line DE. Synthesizing the experience of the 13 National Institute of Food and Agriculture-Conservation Effects Assessment Project Watershed Studies: present and future. In: Osmond DL, Meals DW, Hoag DLK, Arabi M, editors. How to build better agricultural conservation programs to protect water quality: The National Institute of Food and Agriculture-Conservation Effects Assessment Project Experience. Ankeny: Soil and Water Conservation Society;2012. pp.151-67.
- Plan de Acción Santa Lucía: medidas de segunda generación. Montevideo: GNA; 2018. 95p.
- Tomer MD, Sadler EJ, Lizotte RE, Bryant RB, Potter TL, Moore MT, Veith TL, Baffaut C, Locke MA, Walbridge MR. A decade of conservation effects assessment research by the USDA Agricultural Research Service: Progress overview and future outlook. *J Soil Water Conserv.* 2014;69(5):365-73.
- Brirhet H, Benaabidate L. Comparison of two hydrological models (Lumped And Distributed) over a pilot area of the Issen Watershed In The Souss Basin, Morocco. *Eur Sci J.* 2016;12(18):347. Doi: 10.19044/esj.2016.v12n18p347.
- Paudel M, Nelson EJ, Downer CW, Hotchkiss R. Comparing the capability of distributed and lumped hydrologic models for analyzing the effects of land use change. *J Hydroinformatics.* 2011;13(3):461-73.
- Arnold JG, Srinivasan R, Muttiah RS, Williams JR. Large area hydrologic modeling and assessment part I: model development. *J Am Water Resour Assoc.* 1998;34(1):73-89. Doi: 10.1111/j.1752-1688.1998.tb05961.x.
- Mer F, Vervoort RW, Baethgen W. Building trust in SWAT model scenarios through a multi-institutional approach in Uruguay. *SESMO.* 2020;2:17892. Doi: 10.18174/sesmo.2020a17892.
- Aznarez C, Jimeno-Sáez P, López-Ballesteros A, Pacheco JP, Senent-Aparicio J. Analysing the impact of climate change on hydrological ecosystem services in Laguna del Sauce (Uruguay) using the SWAT Model and Remote Sensing Data. *Remote Sens (Basel).* 2021;13(10):2014. Doi: 10.3390/rs13102014.
- Vilaseca F, Castro A, Chreties C, Gorgoglione A. Daily rainfall-runoff modeling at watershed scale: a comparison between physically-based and data-driven models. In: *Computational Science and Its Applications – ICCSA 2021.* Berlin: Springer-Verlag; 2021. pp.18-33.
- Gelós M, Neighbor N, Kok P, Badano L, Hastings F, Nervi E, Alonso J, Navas R, Vervoort W, Baethgen W. On the prediction of phosphorus fluxes in the Santa Lucía basin under different land use and management practices using SWAT model. In: *Phosphorus in Soils and Plants Symposium towards a sustainable phosphorus utilization in agroecosystems.* Montevideo: Facultad de Agronomía; 2022. pp. 81.

16. Hastings F, Kok P, Gelós M, Tejera Á. Implementación de un modelo de calidad de agua con la herramienta SWAT en la cuenca del Río Negro. In: XI Congreso Nacional de AIDIS [Internet]. Montevideo: AIDISUruguay;2022 [cited 2023 Dec 19]. 8p. Available from: <https://aidis.org.uy/wp-content/uploads/2022/11/Hastings-Florencia.pdf>
17. Nervi E, Gelós M, Kok P, Alonso J, Navas R, Badano L, Neighbor N, Hastings F, Vervoort RW, Baethgen W. Evaluación de escenarios de uso del suelo en una subcuenca del río Santa Lucía utilizando el modelo SWAT. In: XI Congreso Nacional de AIDIS [Internet]. Montevideo: AIDIS Uruguay; 2022 [cited 2023 Dec 19]. 8p. Available from: <https://aidis.org.uy/wp-content/uploads/2022/11/Nervi-Eliana-2.pdf>
18. Arnold JG, Youssef MA, Yen H, White MJ, Sheshukov AY, Sadeghi AM, Moriasi AM, Steiner JL, Amatya D, Skaggs RW, Haney EB, Jeong J, Arabi M, Gowda PH. Hydrological processes and model representation: impact of soft data on calibration. *Trans ASABE*. 2015;58(6):1637-60.
19. Nelson AM, Moriasi DN, Talebizadeh M, Steiner JL, Gowda PH, Starks PJ, Tadesse HK. Use of soft data for multicriteria calibration and validation of Agricultural Policy Environmental eXtender: impact on model simulations. *J Soil Water Conserv*. 2018;73(6):623-36.
20. Hastings F, Fuentes I, Perez-Bidegain M, Navas R, Gorgoglione A. Land-cover mapping of agricultural areas using machine learning in Google Earth Engine. In: International Conference on Computational Science and Its Applications. Cham: Springer;2020.pp. 721-36.
21. Climate-Smart Agriculture in Uruguay [Internet]. Washington: The World Bank Group; 2015 [cited 2023 Dec 04]. Available from: <https://climateknowledgeportal.worldbank.org/sites/default/files/2019-06/CSA%20in%20Uruguay.pdf>
22. Ministerio de Ganadería, Agricultura y Pesca (UY). Uruguay agointeligente: los desafíos para un desarrollo sostenible. Montevideo: MGAP; 2017. 161p.
23. Hastings F, Perez-Bidegain M, Navas R, Gorgoglione A. Impacts of irrigation development on water quality in the San Salvador watershed (Part 2): implementation of scenarios in SWAT. *Agrociencia Uruguay*. *Agrociencia Urug*. 2023;27(NE1):e1199. Doi: 10.31285/AGRO.27.1199.
24. Instituto Nacional de Estadística. Resultados del Censo de Población 2011: población, crecimiento y estructura por sexo y edad. Montevideo: INE; 2012. 17p.
25. Instituto Uruguayo de Meteorología. Clasificación climática [Internet]. Montevideo: INUMET; [cited 2023 Jul 18]. Available from: <https://www.inumet.gub.uy/clima/estadisticas-climatologicas/clasificacion-climatica>
26. Pedro A, Macarena C, Cintia P. Análisis del agro-negocio como forma de gestión empresarial en América del Sur: el caso uruguayo. *Agrociencia Uruguay*. 2012;16(1):110-9. Doi: 10.31285/AGRO.17.546.
27. Ministerio de Ganadería, Agricultura y Pesca (UY). Censo General Agropecuario 1990. Montevideo: DCE; 1994. 239p.
28. Ministerio de Ganadería, Agricultura y Pesca, DIEA (UY). Anuario Estadístico Agropecuario 2021. Montevideo: MGAP; 2022. 263p.
29. Petraglia C, Dell'Acqua M, Pereira G, Yussim E. Mapa integrado de cobertura / uso del suelo del Uruguay, año 2018. In: Anuario OPYPA 2019. Montevideo: MGAP; 2019. pp. 523-31.
30. Neitsch S, Arnold JG, Kiniry JR, Williams JR. Soil and water assessment tool. Temple: Texas A&M University; 2011. 618p.
31. Infraestructura de datos espaciales [Internet]. Montevideo: IDEUY; [cited 2023 Jul 18]. Available from: [https://visualizador.ide.uy/ideuy/core/load\\_public\\_project/ideuy/](https://visualizador.ide.uy/ideuy/core/load_public_project/ideuy/)
32. Ministerio de Ganadería, Agricultura y Pesca, DGRN (UY). Carta de suelos escala 1:40,000 [Internet]. Montevideo: MGAP; [cited 2023 Jul 18]. Available from: <https://dgrn.mgap.gub.uy/js/visores/dgrn/#>
33. Mapa de estaciones del Instituto Uruguayo de Meteorología (INUMET) [Internet]. Montevideo: INUMET; [cited 2023 Jul 18]. Available from: <https://www.inumet.gub.uy/clima/recursos-hidricos/mapa-de-estaciones>
34. INIA. Banco de datos agroclimáticos [Internet]. Montevideo: INIA; [cited 2023 Jul 18]. Available from: <https://bit.ly/2KOj2dZ>
35. Saxton KE, Rawls WJ. Soil water characteristic estimates by texture and organic matter for hydrologic solutions. *Soil Sci Soc Am J*. 2006;70(5):1569-78.



36. Durán A. Clasificación hidrológica de los suelos del Uruguay. *Agrociencia Uruguay* 1997;1(1):15-29. Doi: 10.31285/AGRO.01.1009.
37. Perdomo C, Barbazán M, Durán JM. Nitrógeno [Internet]. Montevideo: Facultad de Agronomía; [cited 2023 Jul 18]. 70p. Available from: <http://www.fagro.edu.uy/fertilidad/publica/Tomo%20N.pdf>
38. Hernández J, Otegui O, Zamalvide JP. Formas y contenidos de fósforo en algunos suelos del Uruguay. *Boletín de Investigación*. 1995(43):32p.
39. Gorgoglione A, Silveira L, Eguren G, Rivas N, Hastings F, Saracho A, Rosas F, Pérez A, Basile F, Carriquiry M, Tiscornia G, Cal A, Navas R, García C, Otero A, Roel A, Vilaseca F, Rodríguez R, Pastorini M, Chreties C, Alonso J, Baethgen W, Ancev T, Vervoot RW, Nervi E, Rosas F. Plataforma para el soporte a la toma de decisión en el desarrollo de la agricultura irrigada sostenible (DAIS-STD) [Internet]. [Place unknown]: OSF; 2023 [cited 2023 Dec 18]. Available from: <https://osf.io/yt9n9g/>
40. Ministerio de Ambiente, DINAGUA (UY). Visualizadores geográficos de DINAGUA [Internet]. Montevideo: MA; [cited 2023 Jul 18]. Available from: [https://www.ambiente.gub.uy/informacion\\_hidrica/](https://www.ambiente.gub.uy/informacion_hidrica/)
41. Sikorska AE, Renard B. Calibrating a hydrological model in stage space to account for rating curve uncertainties: general framework and key challenges. *Adv Water Resour*. 2017;105:51-66.
42. Genta JL, Failache N, Alonso J, Bellón D. Balances hídricos superficiales en cuencas del Uruguay. Montevideo: Universidad de la República; 2001. 115p.
43. Tchobanoglous G, Burton FL; Metcalf & Eddy. *Wastewater engineering: treatment, disposal and reuse*. New York: McGraw-Hill; 1991. 1334p.
44. Ministerio de Ganadería, Agricultura y Pesca, SNIG (UY). Datos basados en la declaración jurada de existencias [Internet]. Montevideo: MGAP; [cited 2023 Jul 18]. Available from: <https://www.snig.gub.uy/principal/snig-principal-institucional-indicadores>
45. Ministerio de Vivienda, Ordenamiento Territorial y Medio Ambiente, DINAMA (UY). Evolución de la calidad de agua en la cuenca del río San Salvador: período 2014-2019. Montevideo: MVOTMA; 2020. 77p.
46. Gorgoglione A, Gregorio J, Ríos A, Alonso J, Chreties C, Fossati M. Influence of Land Use/Land Cover on Surface-Water Quality of Santa Lucía River, Uruguay. *Sustainability*. 2020;12(11):4692. Doi: 10.3390/su12114692.
47. Wischmeier WH, Smith DD. Predicting rainfall-erosion losses from cropland east of the Rocky Mountains: guide for selection of practices for soil and water conservation. Washington: USDA; 1965. 47p.
48. Her Y, Frankenberger J, Chaubey I, Srinivasan R. Threshold effects in HRU definition of the soil and water assessment tool. *Trans ASABE*. 2015;58(2):367-78.
49. Williams JR. Sediment yield predictions with universal equation using runoff energy factor. In: *Present and prospective technology for predicting sediment yield and sources*. Washington: USDA; 1975. pp. 244-52.
50. Sadeghi SHR, Gholami L, Khaledi Darvishan A, Saeidi P. A review of the application of the MUSLE model worldwide. *Hydrol Sci J*. 2014;59(2):365-75.
51. Clericci C, Préchac F. Aplicaciones del modelo USLE/RUSLE para estimar pérdidas de suelo por erosión en Uruguay y la región sur de la cuenca del Río de la Plata. *Agrociencia*. 2001;5(1):92-103.
52. Brown L, Barnwell T. *The Enhanced Stream Water Quality Models QUAL2E and QUAL2E-UNCAS (EPA/600/3-87-007)*. Athens: Environmental Research Laboratory; 1987. 188p.
53. Nair SS, King KW, Witter JD, Sohngen BL, Fausey NR. Importance of crop yield in calibrating watershed water quality simulation tools. *J Am Water Resour Assoc*. 2011;47(6):1285-97.
54. Saltelli A, Tarantola S, Chan KPS. A Quantitative model-independent method for global sensitivity analysis of model output. *Technometrics*. 1999;41(1):39-56.
55. Abbaspour KC, Johnson CA, van Genuchten MTh. Estimating uncertain flow and transport parameters using a sequential uncertainty fitting procedure. *Vadose Zone J*. 2004;3(4):1340-52.
56. Kennedy J, Eberhart R. Particle swarm optimization. In: *Proceedings of ICNN'95 - International Conference on Neural Networks*; 1995 Nov 27 – Dec 1; Perth, WA, Australia. Perth: IEEE; 1995. pp. 1942-8.



57. Abbaspour KC, Rouholahnejad E, Vaghefi S, Srinivasan R, Yang H, Kløve B. A continental-scale hydrology and water quality model for Europe: calibration and uncertainty of a high-resolution large-scale SWAT model. *J Hydrol.* 2015;524:733-52.
58. Nossent J, Bauwens W. Multi-variable sensitivity and identifiability analysis for a complex environmental model in view of integrated water quantity and water quality modeling. *Water Sci Technol.* 2012;65(3):539-49.
59. Schuerz C. SWATrunR: Running SWAT2012 and SWAT+ Projects in R. R package version 0.2.7 [Internet]. California: Github; 2019 [cited 2023 Aug 23]. Available from: <https://github.com/chrisschuerz/SWATplusR>
60. Nash JE, Sutcliffe JV. River flow forecasting through conceptual models part I: a discussion of principles. *J Hydrol.* 1970;10(3):282-90.
61. Gupta HV, Kling H, Yilmaz KK, Martinez GF. Decomposition of the mean squared error and NSE performance criteria: implications for improving hydrological modelling. *J Hydrol.* 2009;377(1-2):80-91.
62. Moriasi DN, Arnold JG, Liew MW Van, Bingner RL, Harmel RD, Veith TL. Model evaluation guidelines for systematic quantification of accuracy in watershed simulations. *Trans ASABE.* 2007;50(3):885-900.
63. Knoben WJM, Freer JE, Woods RA. Inherent benchmark or not? Comparing Nash-Sutcliffe and Kling-Gupta efficiency scores. *Hydrol Earth Syst Sci.* 2019;23(10):4323-31. Doi: 10.5194/hess-2019-327.
64. Perdomo C. Metodología de estimación de aportes difusos de nitrógeno y fósforo a aguas superficiales desde suelos bajo uso agropecuario. Montevideo: MA; 2013. 6p.
65. Ministerio de Ganadería, Agricultura y Pesca, DGRN (UY). Estimación de fósforo index [Internet]. Montevideo: MGAP; 2022[cited 2023 Dec 18]. Available from: <https://bit.ly/4aM1tCO>
66. U.S. Environmental Protection Agency. An approach for using load duration curves in the development of TMDLs [Internet]. Washington: Watershed Branch; 2007[cited 2023 Dec 18]. 68p. Available from: <https://bit.ly/3TEtjKQ>
67. Aubriot L, Chalar G, De León L, Goyenola G, Lizarralde C, Míguez B, Perdomo C, Quintans F, Rodó E, Teixeira de Mello F. Establecimiento de niveles guía de estado trófico en cuerpos de agua superficiales. Montevideo: MA; 2017. 48p.
68. Seibert J. On the need for benchmarks in hydrological modelling. *Hydrol Process.* 2001;15(6):1063-4.
69. Her Y, Yoo SH, Cho J, Hwang S, Jeong J, Seong C. Uncertainty in hydrological analysis of climate change: multi-parameter vs. multi-GCM ensemble predictions. *Sci Rep.* 2019;9(1):4974. Doi: 10.1038/s41598-019-41334-7.
70. Liu L, Wang QJ, Xu YP. Temporally varied error modelling for improving simulations and quantifying uncertainty. *J Hydrol.* 2020;586:124914. Doi: 10.1016/j.jhydrol.2020.124914.
71. García JA. Producción de forraje de pasturas cultivadas en la Región Litoral Sur. In: Risso D, Berretta E, Morón A, editors. Producción y manejo de pasturas. Montevideo: INIA; 1996. pp.163-8.



## Supplementary material

Table S1. Data description and sources

Dataset	Format	Resolution	Period	Source
Digital Elevation Model	Raster	0.32 m/ pixel resized to 120 m/pixel	2019	Spatial Data Infrastructure - Agency for the Development of Electronic Management and the Information and Knowledge Society (IDE-AGESIC).
Land Use/Cover Map	Raster	30 m/ pixel resized to 120 m/pixel	1990	Hastings and others <sup>(20)</sup>
Land Use/Cover Map	Raster	10 m/ pixel resized to 120 m/pixel	2018	Petraglia and others <sup>(29)</sup>
Soil Map and soil physical-chemical properties	Shape file and table	esc.: 1:40,000	---	General Directorate of Natural Resources of the Ministry of Livestock, Agriculture, and Fisheries (DGRN-MGAP)
Precipitation Data	Time series	Daily, 13 stations	1988-2021	Uruguay Meteorological Institute (INUMET)
Meteorological Data	Time series	Daily, 1 station	1988-2021	National Agricultural Research Institute (INIA)
Stream flow	Time series	Daily, 1 station	1990-2000	National Water Directorate of the Ministry of Environment (DINAGUA-MA).
Water Quality	Time series	Semesterly, 11 stations	2014-2021	National Environmental Observatory of the Ministry of Environment (OAN-MA)
Agricultural and irrigation management	Table	Annual	---	Consultation with local stakeholders and the group United Irrigators of Uruguay
Crop yields	Time series	Annual	2010-2021	Uruguayan Federation of Regional Agricultural Experimentation (FUCREA)
Irrigated crop yields	Time series	Annual	2010-2021	Consultation with the group United Irrigators of Uruguay.
Grassland biomass	Time series	Annual	2010-2021	DIEA-MGAP <sup>(28)</sup>
Production and native forest biomass	Value	Annual mean	---	Consultation with technicians of the General Forestry Directorate of the Ministry of Livestock, Agriculture, and Fisheries (DGF-MGAP)
Pasture biomass	Value	Annual mean	---	García <sup>(71)</sup>
Sediment yields	Table	Mean annual	2000-2020	General Directorate of Natural Resources of the Ministry of Livestock, Agriculture, and Fisheries (DGRN-MGAP)
Nitrogen and phosphorus yields	Table	Mean annual	Different periods	Perdomo <sup>(64)</sup>

Table S2. Crop rotations associated with Land Use of 1990

ID	Type	% rainfed area	1		2		3	4
AGRC	Rainfed -grazing	14%	Corn	Barley	Sorghum	Winter wheat	Pasture	Pasture
AGRP		86%	Pasture	Winter wheat	Oats	Winter wheat	Pasture	Pasture

AGR1, AGR2, AGR3, AGR4, and AGRP belong to rainfed agriculture with the proportions indicated in the table; AGRP includes a three-year grazing pasture, and AGR1 represents irrigated agriculture.

Table S3. Crop rotations associated with Land Use of 2018

ID*	Type	% rainfed area	1		2		3		4	5
AGR1	Rainfed	37%	W. wheat	Soyb. 2nd	Oats	Soyb. 1st				
AGR2		18%	Barely	Soyb. 2nd	W. wheat	Soyb. 2nd				
AGR3		27%	Oats	Corn 1st	Oats	Soyb. 1st				
AGR4		9%	W. wheat	Soyb. 2nd	Oats	Corn 1st	Oats	Soyb. 1st		
AGRP	Rainfed -grazing	9%	Pasture	Soyb. 1st	Oats	Soyb. 1st	Pasture	Pasture	Pasture	Pasture
AGRI	Irrigated	---	Oats	Soyb. 1st	Oats	Soyb. 1st	Oats	Corn 1st		

\*1<sup>st</sup> and 2<sup>nd</sup> refer to the fact that a cover crop and a winter crop, respectively, were planted before this crop.

Table S4. Operations for the management of crops

Crop*	Planting	Harvest	Irrigation	Fertilization (Kg/ha/season)	
				Nitrogen	Phosphorus
Barley / Winter wheat	14-Jun	25-Nov	No	92	46
Corn 1 <sup>st</sup>	23-Sep	20-Feb	No	119	69
Corn 2 <sup>nd</sup>	10-Dec	15-May	No	119	69
Soybean 1 <sup>st</sup>	12-Nov	21-Apr	No	0	20
Soybean 2 <sup>nd</sup>	10-Dec	1-May	No	0	20
Corn	23-Sep	20-Feb	Yes	215	79
Soybean	12-Nov	21-Apr	Yes	0	24
Pasture**	22-Apr	11-Nov	No	27	69

\*1<sup>st</sup> and 2<sup>nd</sup> refer to the fact that a cover crop and a winter crop, respectively, were planted before this crop. \*\*The pasture has a duration of three years, is fertilized at planting as indicated in the table and then re-fertilized each year with 14 kg N/ha and 37 kg P/ha, and also receives additional organic fertilizer through grazing.

Table S5. Parameters for soft calibration of plants. Bibliographic ranges, default values in SWAT, and final set parameters. Part 1

Parameter	Definition	Production forest			Native forest			Pasture			Native grasses		
		Biblio.	Default	Final	Biblio.	Default	Final	Biblio.	Default	Final	Biblio.	Default	Final
BIO_E	Biomass/Energy Ratio ((kg/ha)/(MJ/m <sup>2</sup> ))	7-75	15	75	---	25	40	2.3-7	35	10	4-12	34	8.5
HVSTI	Harvest index	0.7	0.76	0.7	---	0.1	0.1	0-0.6	0.9	0.9	---	0.9	0.9
BLAI	Max leaf area index	3.5	5	3.5	---	5	5	---	4	4	---	2.5	4
CHTMX	Max canopy height (m)	20	6	20	---	5.9	6.2	---	0.5	0.6	---	1	0.4
RDMX	Max root depth (m)	3	3.5	3	---	2.5	2.5	---	2	2	---	2	2
T_OPT	Min temp plant growth (°C)	20	30	19	---	17	17	20-25	25	19	---	25	17
T_BASE	Optimal temp for plant growth (°C)	7	10	6	---	1	1	2-5	12	6	---	12	2.5
BN1	Fraction of N in plant at emergence (kg N/kg biomass)	---	0.006	0.004	---	0.003	0.002	---	0.06	0.025	---	0.02	0.003
BN2	Fraction of N in plant at 50% maturity (kg N/kg biomass)	---	0.002	0.001	---	0.001	5E-04	---	0.023	0.013	---	0.012	0.003
BN3	Fraction of N in plant at maturity (kg N/kg biomass)	---	0.002	7E-04	---	7E-04	5E-04	---	0.013	0.006	---	0.005	0.001
ALAI_MIN	Minimum leaf area index for plant during dormant period (m <sup>2</sup> /m <sup>2</sup> )	2	0.75	2	---	2	2	---	0	1	---	0	1
MAT_YRS	Number of years for trees to reach full development (years)	9	50	9	---	50	10	---	0	0	---	0	0
BMX_TRES	Maximum biomass for a forest (Mg/ha)	260	1000	260	---	140	127	---	0	0	---	0	0



Table S6. Parameters for soft calibration of plants. Bibliographic ranges, default values in SWAT, and final set parameters. Part 2

Parameter	Soybean 1 <sup>st</sup> and 2 <sup>nd</sup>				Corn 1 <sup>st</sup>				Winter Wheat			Spring Barley			Oats		
	Biblio.	Default	Final	Final Irr.	Biblio.	Default	Final	Final Irr.	Biblio.	Default	Final	Biblio.	Default	Final	Biblio.	Default	Final
BIO_E	14-29	25	20	22	17-49	39	32	45	17-36	30	22	12-35	35	23	14-47	35	25
HVSTI	0.3-0.5	0.31	0.35	0.35	0.45-0.47	0.5	0.45	0.45	0.35-0.43	0.4	0.4	0.4-0.5	0.54	0.4	0.4-0.7	0.42	0.42
BLAI	6-6.5	3	6	6.5	5.7-6.5	6	5.8	6.5	7	4	6	7	4	6		4	4
CHTMX	---	0.8	0.8	0.8	---	2.5	2.5	2.5	---	0.9	0.8	---	1.2	0.8		1.5	1.25
RDMX	---	1.7	0.75	0.75	---	2	2	2	---	1.3	0.8	---	1.3	0.7		2	1
T_OPT	27.5-28	25	27.8	27.8	34	25	30	30	8-25	18	18	24.5	25	24.5	26	15	15
T_BASE	5-7	10	6	6	8	8	8	8	0	0	0	0	0	0	2	0	0

Table S7. SWAT parameters considered for the flow sensitivity analysis

Parameter	Definition	Process	Filter LU*	Default values	Sensitivity range
CN2.mgt	SCS runoff curve number for moisture condition II	Surface runoff	A	49 to 87	-20 to 15%
			B	45 to 83	-20 to 15%
ESCO.hru	Soil evaporation compensation factor	Evapotranspiration	A	0.95	0.3 to 1
			B	0.95	0.3 to 1
OV_N.hru	Manning's "n" value for overland flow	Surface runoff	A	0.15 and 0.3	-90 to 500%
			B	0.1 and 0.14	-90 to 500%
HRU_SLP.hru	Average slope steepness (m/m)	Surface runoff	---	0.0001 to 0.1007	-30 to 30%
SLSUBBSN.hru	Average slope length (m)	Concentration time, sediment erosion	---	61, 91, 122	-70% to 200%
CANMX.hru	Maximum canopy index (mm)	Evapotranspiration	A	1.5	1 to 3
			B	3.5	3 to 8
ALPHA_BF.gw	Base flow recession factor (1/day)	Groundwater	---	0.1	0 to 1
GW_DELAY.gw	Groundwater delay (days)	Groundwater	---	31	0 to 300
GW_REVAP.gw	Groundwater 'revap' coefficient	Groundwater	---	0.02	0.02 to 0.2
GWQMN.gw	Threshold depth of water in shallow aquifer for return flow to occur (mm)	Groundwater	---	1000	100 to 5000
REVAPMN.gw	Threshold depth of water in the shallow aquifer for 'revap' (mm)	Groundwater	---	750	100 to 1000
RCHRG_DP.gw	Groundwater recharge to deep aquifer (fraction)	Groundwater	---	0.02	0 to 0.15
SOL_AWC.sol	Available water capacity of the soil layer (mm/mm soil)	Soil water	---	0.08 to 0.19	0 to 300%
SURLAG.bsn	Surface runoff lag coefficient	Surface runoff	---	4	0 to 72
CH_N2.rte	Manning coefficient for channel	Routing	---	0.05	0.015 to 0.150
CH_L2.rte	Length of main channel (km)	Routing	---	8 to 59	-50 to 100%
CH_S2.rte	Average slope of main channel (m/m)	Routing	---	0.0006 to 0.0021	-50 to 100%
CH_K2.rte	Effective hydraulic conductivity in main channel alluvium (mm/h)	Routing	---	6	0.0001 to 25



Table S8. Observed water quality, 2014-2021. #: quantity of samples

Station	Start	TP (mg/L)			TN (mg/L)			TSS (mg/L)					
		#	Prom.	Max.	Min.	#	Prom.	Max.	Min.	#	Prom.	Max.	Min.
SS10	May-14	38	0.20	0.59	0.04	18	1.5	3.8	0.3	40	17	210	3
SS20	May-14	36	0.32	0.80	0.08	18	1.6	4.7	0.8	40	20	110	3
SS30	May-14	35	0.35	0.73	0.13	17	1.4	2.0	0.7	39	16	97	3
SS40	May-14	38	0.36	0.63	0.15	19	1.6	2.8	0.8	39	18	84	4
SS50	May-14	38	0.39	1.40	0.13	18	2.7	16.0	1.0	40	36	670	5
SS60	May-14	36	0.37	0.77	0.13	19	1.8	3.5	0.8	40	19	160	3
SS70	May-14	36	0.39	0.78	0.17	20	1.8	3.5	1.0	40	20	130	3
AG100	May-19	13	0.42	1.19	0.11	2	3.1	4.2	1.9	14	14	50	4
MA90	May-19	14	0.41	0.71	0.13	1	4.0	4.0	4.0	14	19	73	5
MG110	May-19	13	0.22	0.57	0.05	2	3.6	6.1	1.1	14	15	84	3
SMA80	May-19	14	0.31	0.62	0.10	2	2.1	3.3	0.9	14	12	66	3

Table S9. Simulated (2014-2021) mean and standard deviation of yields from Sediments (SYLD), Total Nitrogen (TN) and Total Phosphorus (TP), for each sub-basin and land use category

Land use	Sub-basin												
	1	2	3	4	5	6	7	8	9	10	11	12	13
<b>SYLD (ton/ha/yr)</b>													
Irrigated cropland	1.43	---	3.66	4.35	---	2.74	2.86	---	2.99	1.56	3.26	2.18	3.94
Rain-fed cropland	2.14	1.82	2.65	2.06	2.05	2.96	2.45	2.96	2.66	2.37	2.63	2.72	2.28
Cropland with grazing	2	2.2	2.35	2.43	2.05	3.7	2.3	3.52	2.74	3.1	2.25	3.29	2.21
Production forest	---	---	0.15	0.14	---	0.29	0.28	0.29	0.06	0.13	---	---	0.16
Native forest	0.03	0.03	0.04	0.03	---	0.15	0.11	0.16	0.04	0.12	0.11	0.04	0.04
Native grassland	0.66	0.66	0.81	0.59	0.95	1.54	1.07	1.62	1.03	1.06	1.31	1.01	0.85
Urban area	---	2.6	---	---	---	---	---	1.06	---	---	---	---	2.25
<b>TP exported (kg/ha/yr)</b>													
Irrigated cropland	1.43	---	3.66	4.35	---	2.74	2.86	---	2.99	1.56	3.26	2.18	3.94
Rain-fed cropland	2.14	1.82	2.65	2.06	2.05	2.96	2.45	2.96	2.66	2.37	2.63	2.72	2.28
Cropland with grazing	2	2.2	2.35	2.43	2.05	3.7	2.3	3.52	2.74	3.1	2.25	3.29	2.21
Production forest	---	---	0.15	0.14	---	0.29	0.28	0.29	0.06	0.13	---	---	0.16
Native forest	0.03	0.03	0.04	0.03	---	0.15	0.11	0.16	0.04	0.12	0.11	0.04	0.04
Native grassland	0.66	0.66	0.81	0.59	0.95	1.54	1.07	1.62	1.03	1.06	1.31	1.01	0.85
Urban area	---	2.6	---	---	---	---	---	1.06	---	---	---	---	2.25
<b>TN exported (kg/ha/yr)</b>													
Irrigated cropland	9.1	---	21.5	22.7	---	16.1	18.2	---	19.2	8.5	19.9	11.7	23.7
Rain-fed cropland	11.6	9.4	13.9	10.4	11.1	15.5	12.8	13.7	14.7	11.4	14	13.4	12.1
Cropland with grazing	7.2	8.3	8.8	9	6.2	14.6	7.6	12.5	9.6	11.3	7.9	12.6	8
Production forest	---	---	0.2	0.2	---	0.4	0.5	0.4	0.1	0.2	---	---	0.1
Native forest	0	0	0	0	---	0	0	0.1	0	0	0	0	0
Native grassland	1.3	1.1	1.6	1	1.6	3.2	2.1	3.2	2.1	2.1	2.6	2.2	1.8
Urban area	---	0.5	---	---	---	---	---	7	---	---	---	---	6.5
<b>Area (ha)</b>													
Irrigated cropland	85	---	619	30	---	439	338	---	72	1	293	747	200
Rain-fed cropland	7111	3128	16954	9942	3924	9856	19694	16454	1684	9262	14536	14864	8154
Cropland with grazing	703	309	1677	983	388	975	1948	1627	166	916	1438	1470	806
Production forest	---	---	3607	876	---	849	436	838	589	566	---	---	1
Native forest	322	346	604	587	---	272	421	371	251	725	863	681	284
Native grassland	1976	535	8252	6885	1567	8038	11296	12701	1956	8533	8523	3382	1296
Urban area	---	529	---	---	---	---	---	1	---	---	---	---	1



Table S10. Point sources of nutrients, annual mean loads of total nitrogen (TN) and total phosphorus (TP)

Land use	Sub-basin												
	1	2	3	4	5	6	7	8	9	10	11	12	13
<b>TP (ton/yr)</b>													
Domestic sewage	0.00	3.29	0.00	0.00	0.00	0.00	0.00	0.00	0.00	0.00	0.00	0.00	0.00
Dairies	0.96	0.24	1.82	0.78	1.38	2.47	3.52	6.67	0.08	0.31	0.44	1.42	0.80
Fattening farms	0.51	0.18	1.11	1.02	0.00	0.22	1.65	0.46	0.10	0.41	0.65	1.27	0.20
<b>TN (ton/yr)</b>													
Domestic sewage	0.0	42.0	0.0	0.0	0.0	0.0	0.0	0.0	0.0	0.0	0.0	0.0	0.0
Dairies	3.7	1.0	6.8	3.3	5.3	9.6	13.9	25.6	0.4	1.5	2.3	5.2	2.9
Fattening farms	2.6	1.0	5.7	5.3	0.0	1.2	8.5	2.4	0.5	2.1	3.3	6.5	1.0

Table S11. Direct sources of nutrients (from unrestricted cattle access to watercourses), annual mean loads of total nitrogen (TN) and total phosphorus (TP)

Land use	Sub-basin												
	1	2	3	4	5	6	7	8	9	10	11	12	13
<b>TP (ton/yr)</b>													
Native grassland	0.51	0.14	2.13	1.78	0.40	2.08	2.92	3.28	0.51	2.20	2.20	0.87	0.33
Cropland with grazing	0.67	0.30	1.61	0.94	0.37	0.93	1.87	1.56	0.16	0.88	1.38	1.41	0.77
<b>TN (ton/yr)</b>													
Native grassland	4.0	1.1	16.8	14.0	3.2	16.4	23.0	25.9	4.0	17.4	17.4	6.9	2.6
Cropland with grazing	5.3	2.3	12.7	7.4	2.9	7.4	14.7	12.3	1.3	6.9	10.9	11.1	6.1

Table S12. Proportional contribution of each source to nutrient loading by flow condition, 2014-2021

Source type	Flow condition source	TN (%)					TP (%)				
		High	Moist	Mid-range	Dry	Low	High	Moist	Mid-range	Dry	Low
Diffuse	Rain-fed cropland	80.6%	59.8%	4.2%	0.6%	0.1%	69.1%	58.5%	2.4%	0.1%	0.0%
	Native grasslands	8.7%	4.7%	2.8%	0.6%	0.1%	19.9%	10.0%	0.3%	0.0%	0.0%
	Cropland with grassland	6.2%	3.8%	0.4%	0.1%	0.1%	7.5%	5.3%	0.1%	0.0%	0.0%
	Irrigated cropland	2.2%	1.8%	0.1%	0.0%	0.0%	1.7%	1.5%	0.1%	0.0%	0.0%
	Other land uses	0.3%	0.0%	0.0%	0.1%	0.0%	0.5%	0.1%	0.0%	0.0%	0.0%
Direct	Grazing on native grasslands	0.9%	12.7%	38.6%	41.0%	41.7%	0.5%	8.2%	31.8%	32.4%	32.3%
	Grazing on cropland	0.5%	7.6%	23.8%	25.0%	25.0%	0.3%	4.9%	19.5%	19.8%	19.4%
Point	Dairies	0.4%	6.3%	19.7%	21.0%	21.2%	0.5%	8.3%	32.7%	33.7%	34.3%
	Fattening farms	0.2%	3.3%	10.4%	11.6%	11.8%	0.2%	3.3%	13.1%	14.0%	14.0%